

# ESTIMATION OF CURIE-POINT ISOTHERM DEPTHS FOR GEOTHERMAL POTENTIAL OF PARTS OF CENTRAL NIGERIA

<sup>1</sup>Isa Hassan Yahaya, <sup>2</sup>Abdullahi Nasir Khalid, <sup>2</sup>Matoh Dary Dogara, <sup>2</sup>Hussaini Abdulkareem, <sup>3</sup>Abdulhadi Danlami

<sup>1</sup>Department of Scientific and Industrial Research, National Research Institute for Chemical Technology (NARICT), Zaria, Kaduna State, Nigeria

<sup>2</sup>Department of Physics, Kaduna State University, Kaduna State, Nigeria

<sup>3</sup>Department of Physics with Electronics, Nuhu Bamalli Polytechnic, Zaria, Kaduna State, Nigeria

\*Corresponding Author Email Address: [inbox2hassan@gmail.com](mailto:inbox2hassan@gmail.com)

## ABSTRACT

An estimation of curie point depths (CPDs), corresponding geothermal gradients (GG), and heat flow (q) was carried out from six High Resolution Aeromagnetic (HRAM) data of parts of central Nigeria using the spectral centroid analysis method. The HRAM was divided into 28 overlapping spectral blocks, and each block was analysed to obtain depths to the top ( $Z_t$ ), centroid ( $Z_0$ ), and bottom ( $Z_b$  or CPD) of the magnetic sources, respectively. Using these values, the corresponding values of geothermal gradient and heat flow were equally determined for the study area. The result shows that CPD varies between 8.95 km and 24.63 km with an average of 16.33 km, the GG between 22.42 °C/km to 61.77 °C/km with an average of 35.52 °C/km, while the heat flow varies between 56.04 mW/m<sup>2</sup> to 154.42 mW/m<sup>2</sup> with an average of 88.80 mW/m<sup>2</sup>, which is within the required heat to generate geothermal energy. Geothermal energy is a promising, sustainable alternative to hydro energy and fossil fuels. Therefore, considering the current energy challenge bedeviling Nigeria, this study is important for assessing the geothermal potential and possible suitability of the study area for geothermal energy generation to contribute towards mitigating Nigeria's energy challenge.

**Keywords:** Curie Point Depth, Geothermal Potential, Data, Spectral Analysis, North Central Nigeria

## INTRODUCTION

Nigeria has long struggled with unreliable power supply due to the unsustainable nature of its primary energy sources: hydroelectric and fossil fuel-based power generation. Hydroelectric power, which depends on seasonal water availability, suffers from fluctuations in output during dry seasons (Jimah, 2019). Meanwhile, fossil fuels, apart from being non-renewable, contribute to environmental pollution through greenhouse gas emissions, exacerbating climate change and ozone layer depletion (Byerly & Stolt, 1977; Glassley, 2010). Despite these challenges, Nigeria remains heavily reliant on these energy sources, limiting the exploration of more sustainable alternatives.

Among renewable energy options, geothermal energy presents a promising solution. Unlike solar or wind power, geothermal energy provides consistent, year-round electricity with minimal greenhouse gas emissions (Dipippo & Renner, 2014). Geothermal resources arise from the Earth's internal heat, driven by mantle plumes, radioactive decay, and residual planetary formation energy (Nemzer, 2009; GEA, 2012). Nigeria's geothermal potential remains largely untapped, despite its advantages over conventional energy sources (Odidi et al., 2020).

Geophysical methods, particularly magnetic surveys, play a crucial role in locating geothermal reservoirs. The Curie point depth—

where minerals lose magnetic properties due to high temperatures—serves as a key indicator of subsurface heat (Stacey, 1977; Langel & Hinze, 1998). Aeromagnetic data, collected via aircraft-mounted magnetometers, offers an efficient means of mapping these thermal structures across large areas (Bernadette et al., 2020). This study explores Nigeria's geothermal potential using such geophysical techniques, contributing to the diversification of the nation's energy mix for sustainable development.

## Location and Geology of the Study Area

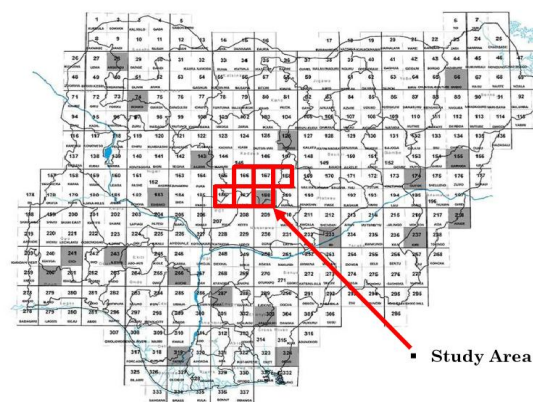


**Figure 1.** A Map of Nigeria Showing the Location of the Study Area (Source: NGSA)

The study area encloses six aeromagnetic sheets (Kachia-166, Kafanchan-167, Naraguta-168, Abuja-186, Gitata-187, and Jemaa-188) covering parts of Kaduna, Abuja, Jos, Nasarawa, and Niger states, within latitudes 8.0°N–10.0°N and longitudes 7.0°E–9.0°E.

**Kachia (Sheet 166)** lies within the Kaduna Plains, characterized by gently undulating terrain with lateritic soils and modified vegetation due to farming and bush burning (Bennett et al., 2013). Geologically, it consists of migmatite (dominant), granite gneiss, schist, quartzites, and biotite (NGSA, 2013; Kehinde et al., 2017).

**Kafanchan (Sheet 167)** straddles Kaduna and Nasarawa states, within the Northern Nigeria Basement Complex, shaped by the Pan-African orogeny (~600 Ma). It features migmatite-gneiss complexes, schist belts, and older granites, with NNE-SSW and

NW-SE strike-slip fault systems (Ogwuche et al., 2021; McCurry, 1971).

**Naraguta (Sheet 168)** covers the Jos Plateau, known for its high elevations (1,800–5,300 m) and rugged topography dominated by younger granites, older granites, and basalts. The plateau's relief is influenced by resistant granites, with basalt formations forming mesas and volcanic cones (Macleod et al., 1971; Akanbi & Mangset, 2011).

**Abuja (Sheet 186)** features undulating hills and inselbergs, including the prominent Zuma Rock, with elevations up to 1,060 m (Akaochere, 2019).

The region's diverse geology and geomorphology, shaped by tectonic events and weathering, provide a valuable setting for geothermal potential assessment using aeromagnetic data.

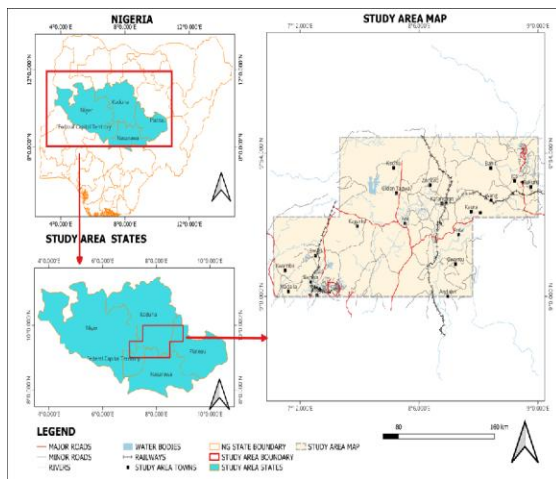


**Figure 2.** A Map Showing the Study Area extracted from the Study Area States. **Author:** Hassan Isa Yahaya

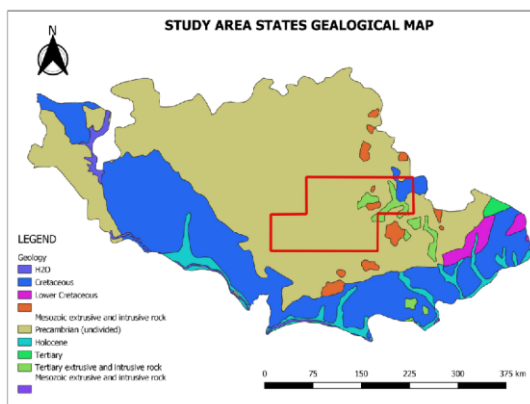


**Figure 3.** Geological Map of the Study Area  
**Author:** Hassan Isa Yahaya

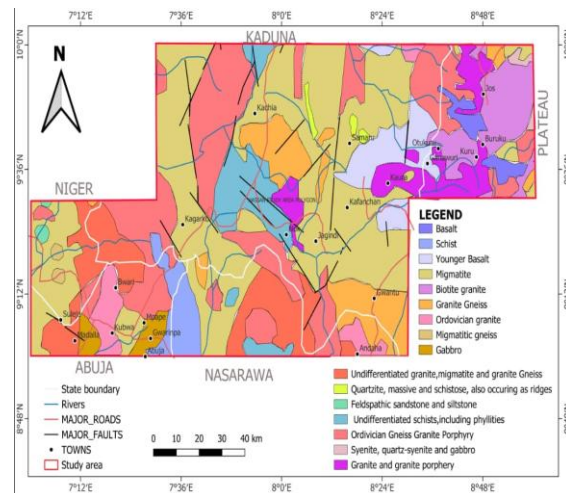


**Figure 4.** Geological Map of the Study Area Showing Lithology  
**Author:** Hassan Isa Yahaya

## METHOD

### Curie Point Depth Estimation

The methods for estimating the Curie depth and determination of geothermal potential have been described by several authors, such as Bhattacharyya and Leu, 1975; Okubo et al., 1985; Onwuemesi, 1997; Tanaka et al., 1999; Stampolidis et al., 2005, and Kasidi & Nur, 2012. However, methods described by Spector & Grant, 1970; Blakely, 1996; and Odidi et al., 2020 are proposed to be used for this work.

The six high-resolution aeromagnetic data (sheets 166, 167, 168, 186, 187, and sheet 188) enclosed within Kachia, Kafanchan, Jema'a, in Kaduna state, and parts of Abuja, Gitata, and Naraguta in Jos were acquired from the Nigerian Geological Survey Agency (NGSA). The survey was conducted by Fugro Airborne Surveys between 2005 and 2010 using 3× Scintrex CS3 cesium vapour magnetometers mounted on Cessna Caravan fixed-wing aircraft at an altitude of 100m along a flight line spacing of 500m, terrain clearance of 80m oriented in NW-SE, and a tie line spacing of 2000m. The data were initially pre-processed by the Fugro Airborne Survey and the consultant team. The pre-processing includes matching each geophysical data with the corresponding global positioning system (GPS), micro levelling, and removal of cultural magnetic effects as a result of artificial features like pipelines, telecommunication cables, railway lines, and others (Mauring, et al., 2002). The projection method used to process the data was the Universal Transverse Mercator (UTM) and the WGS 84 as datum.

Using the Oasis Montaj software, the six high-resolution aeromagnetic data sets obtained were merged into one grid to obtain a single grid for the study area. This grid was then re-projected in the Universal Transverse Mercator (UTM) 32°N geographic coordinate system to obtain the Total Magnetic Intensity (TMI) grid of the study area. Reduction to the Equator (RTE) was carried out with geomagnetic inclination of 1.4° and declination of 1.7°, to centre anomalies over their respective sources, in line with standard magnetic data correction practices for regions such as the study area that are located in low-latitude regions.

The data was then further trend-filtered to eliminate the regional

trends, hence producing the Residual Magnetic Intensity (RMI) data.

The RMI data was further divided into 28 spectral blocks overlapping by 50% and each block was analysed to generate values of spectral power (P) and corresponding wave numbers (k).

### Depth Estimation Using Spectral Analysis

The estimation of the Curie point depth was carried out based on spectral analysis of the residual data. Bhattacharyya & Leu (1975) and Blakely (1996) presented that the depth to bottom (Z<sub>b</sub>) of a magnetic source body could be estimated as follows;

Firstly, is the estimation of depth to the centroid (Z<sub>0</sub>) of the magnetic source from the slope of the longest wavelength part of the spectrum, yielding,

$$\ln P|k|^{1/2} = \ln B - |k|Z_t \quad 1$$

Where B is a constant term. The depth to the top magnetic sources Z<sub>t</sub> was estimated by taking the slope around the high-wave-number part of the radially averaged power spectrum [ $\ln P|k|^{1/2}$ ]

The second step is the estimation of depth to the top boundary (Z<sub>t</sub>) of that distribution from the slope of the second longest wavelength spectral segment (Okubo et al., 1985), thus,

$$\ln \left\{ \frac{P|k|^{1/2}}{|k|} \right\} = \ln D - |k|Z_0 \quad 2$$

Where the term D is a constant. The depth to the center of magnetic sources, Z was estimated by taking the slope around the low wave number part of the radially averaged power spectrum.

Then the basal depth (Z<sub>b</sub>) of the magnetic source will be calculated from the equation below:

$$Z_b = 2Z_0 - Z_t \quad 3$$

The obtained basal depth (Z<sub>b</sub>) of magnetic sources is assumed to be the Curie point depth (Bhattacharyya & Leu, 1975; Okubo et al., 1985).

The geothermal gradient and heat flow value were calculated using the following relations

$$\frac{dT}{dz} = \frac{T_c - T_s}{Z_b} = \frac{580^\circ C - T_s}{Z_b} \quad 4$$

Where T<sub>s</sub>, is the surface temperature. The surface temperatures for the study areas were obtained from data from the World Bank Geoportal on climate.

The heat flow values (q) were calculated using the equation

$$q = k \frac{dT}{dz} = k \left( \frac{580^\circ C - T_s}{Z_b} \right) \quad 5$$

where q is the heat flow and k is the coefficient of thermal conductivity. The k value differs from area to area. The variation in the value of k is a result of the different rock units that are within any given area.

## RESULTS AND DISCUSSION

### Total Area / Dimension of Grid Used

The total area is approximately = 18345.615 square kilometers as calculated using QGIS.

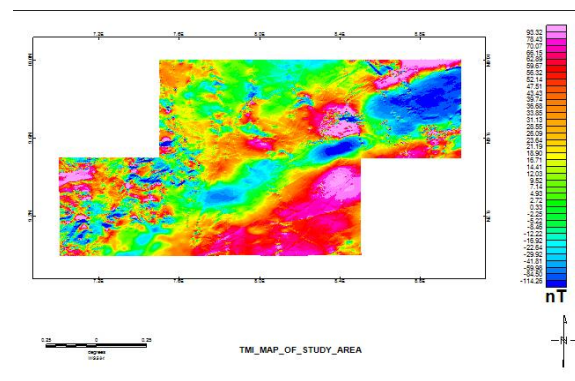


Figure 5. Total Magnetic Intensity (TMI) Map of The Study Area

Figure 5 above shows the Total Magnetic Intensity (TMI) map of the study area before regional and residual separation. This map is a merger of the six aeromagnetic maps used for this research. This was done so that the six maps can be processed unanimously under the same conditions.

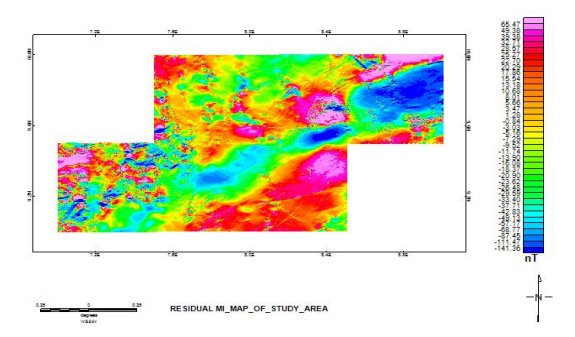


Figure 6. Residual Magnetic Intensity Map of the Study Area

Figure 6. The above is the Residual Magnetic Intensity (RMI) map of the study area, which is free of deeper features present in the original TMI map. It was obtained by filtering the TMI map using the Oasis Montaj software to separate the Residual Magnetic intensity from the Regional Magnetic Intensity. This was done in order to eliminate the deeper features with long wavelength anomalies that are located at distances that are not significant for curie depth investigations. What is required in these investigations are shallow near-surface features, short-wavelength features, and higher frequency components.

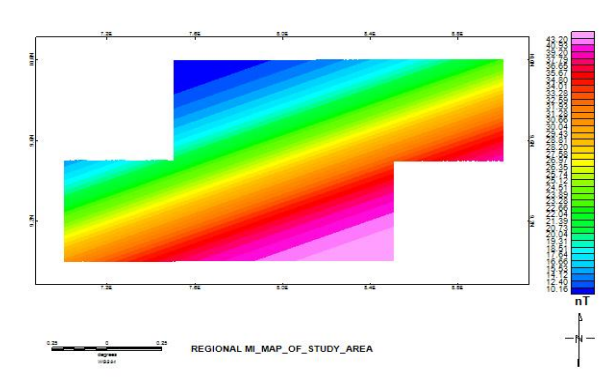


Figure 7. Residual Magnetic Intensity Map of the Study Area



The Regional Magnetic Intensity (RegMI) map of the study area is shown above in Figure 7. This map contains deep-seated geological structures such as crustal thickness variation, faults, or rifts. It also contains long wavelength features, including tectonic fabric and crustal composition, and lower frequency components which are often related to deeper sources.

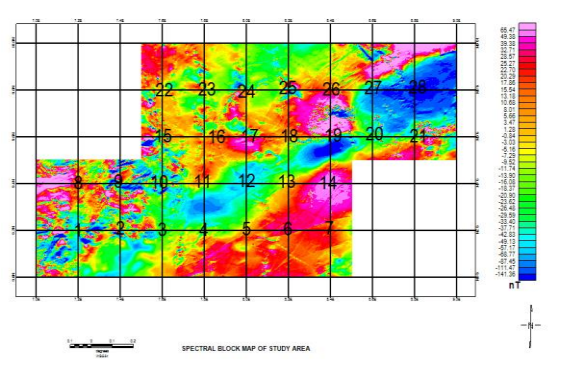


Figure 8. Spectral Blocks Map

The spectral blocks for the study area are shown in Figure 8 above. The area was divided into 28 spectral blocks, which were individually analysed to generate the power spectrum, radial average of the power spectrum, and the depths to the top ( $Z_t$ ) and centroid ( $Z_0$ ), respectively as presented in Table 1. The spectral plots for blocks 1 to 4 of 28 blocks are shown in Figure 9 below.

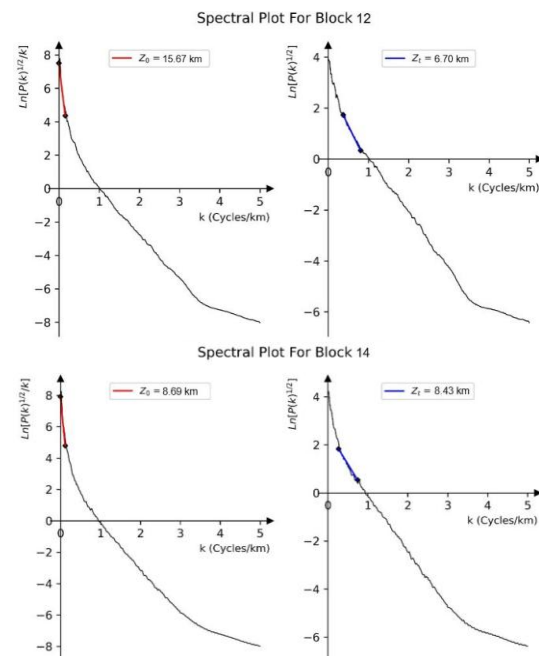


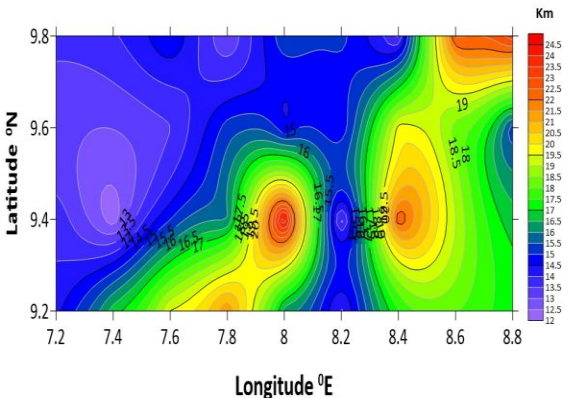
Figure 9. Spectral Plots for Blocks 12 and 14.

Figure 9 above shows the spectral plots for blocks 12 and 14 of the 28-block plotted using equations 1 and 2 from above.

Table 1. Values for Depth to the Centroid ( $Z_0$ ), Top ( $Z_t$ ), Curie Depth ( $Z_b$ ), Geothermal Gradient (GG), and Heat Flow (Q)

BLOCKS	X1	X2	Y1	Y2	LON G. (DEG)	LAT. (DEG)	$Z_0$ (Km)	$Z_t$ (Km)	$Z_b$ (Km)	dT/dZ ( $^{\circ}$ C/Km)	q (mWm $^{-2}$ )
i.	7.0	7.4	9.0	9.4	7.20	9.20	9.78	5.20	14.36	38.47	96.16491548
ii.	7.2	7.6	9.0	9.4	7.40	9.20	9.44	2.10	16.77	32.94	82.36092397
iii.	7.4	7.8	9.0	9.4	7.60	9.20	11.45	3.36	19.53	28.31	70.7708774
iv.	7.6	8.0	9.0	9.4	7.80	9.20	12.90	4.38	21.43	25.80	64.49512769
v.	7.8	8.2	9.0	9.4	8.00	9.20	10.93	5.64	16.21	34.05	85.13233453
vi.	8.0	8.4	9.0	9.4	8.20	9.20	10.05	6.19	13.91	39.69	99.23536517
vii.	8.2	8.6	9.2	9.6	8.40	9.40	13.82	5.20	22.43	24.61	61.53340318
viii.	7.0	7.4	9.2	9.6	7.20	9.40	8.84	3.85	13.83	39.96	99.89379605
ix.	7.2	7.6	9.2	9.6	7.40	9.40	8.22	4.24	12.21	45.24	113.1117357
x.	7.4	7.8	9.2	9.6	7.60	9.40	9.57	4.16	14.98	36.91	92.27148294
xi.	7.6	8.0	9.2	9.6	7.80	9.40	10.20	4.47	15.92	34.72	86.78845961
xii.	7.8	8.2	9.2	9.6	8.00	9.40	15.67	6.70	24.63	22.42	56.04155332
xiii.	8.0	8.4	9.2	9.6	8.20	9.40	10.17	7.08	13.26	41.65	104.1286307
xiv.	8.2	8.6	9.2	9.6	8.40	9.40	8.69	8.43	8.95	61.77	154.4176
xv.	7.4	7.8	9.4	9.8	7.60	9.60	8.37	3.27	13.47	40.91	102.2795597
xvi.	7.6	8.0	9.4	9.8	7.80	9.60	10.09	4.94	15.23	36.18	90.44899567
xvii.	7.8	8.2	9.4	9.8	8.00	9.60	9.20	3.85	14.54	37.90	94.7616002
xviii.	8.0	8.4	9.4	9.8	8.20	9.60	10.00	5.34	14.66	37.59	93.96481178
xix.	8.2	8.6	9.4	9.8	8.40	9.60	12.67	5.63	19.71	28.04	70.09871576
xx.	8.4	8.8	9.4	9.8	8.60	9.60	12.97	7.62	18.31	30.18	75.44095563
xxi.	8.6	9.0	9.4	9.8	8.80	9.60	9.82	4.49	15.16	36.46	91.14562716
xxii.	7.4	7.8	9.6	10.0	7.60	9.80	8.80	2.58	15.02	36.69	91.7291331

xxiii.	7.6	8.0	9.6	10.0	7.80	9.80	8.34	3.68	13.00	42.39	105.9711135
xxiv.	7.8	8.2	9.6	10.0	8.00	9.80	9.46	3.52	15.39	35.81	89.52925506
xxv.	8.0	8.4	9.6	10.0	8.20	9.80	9.42	3.69	15.15	36.39	90.97571604
xxvi.	8.2	8.6	9.6	10.0	8.40	9.80	8.86	4.34	13.38	41.29	103.2350809
xxvii.	8.4	8.8	9.6	10.0	8.60	9.80	13.18	3.76	22.59	24.46	61.14321058
xxviii.	8.6	9.0	9.6	10.0	8.80	9.80	13.78	4.26	23.31	23.71	59.26821682
AVERAGE									16.33	35.52	88.79779277



**Figure 10.** Curie Point Depth Contour Map  
The contour map above shows the curie depth represented against the latitude and longitude of the study area, indicating the depth variations to the base of magnetic sources ( $Z_b$ ) across the study area as represented by contours.

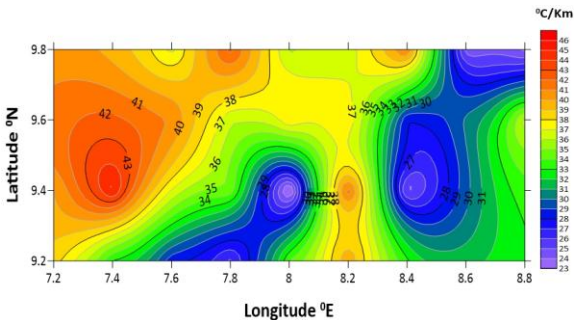


**Figure.** Error! No text of specified style in document. 11 Geothermal Gradient Contour Map

Figure 11 above shows the geothermal gradient represented against the latitude and longitude of the study area, indicating variations of temperature increase per unit depth across the study area as represented by contours.

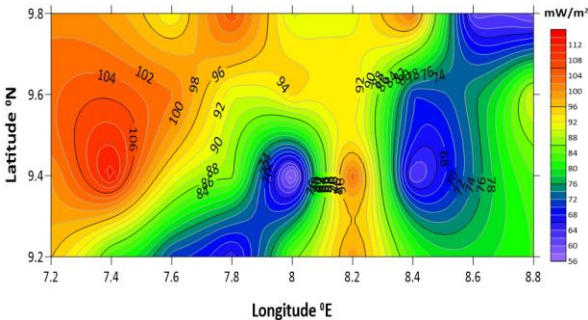


**Figure 12.** Heat Flow Contour Map

The figure above shows the heat flow contour map of the study area. This map shows heat flow values represented against the latitude and longitude of the study area. The map shows variations of heat flow across the study area.

## DISCUSSION

From the results obtained in this study, block 14, which corresponds to areas around Antang and Kaura, showed the shallowest Curie depths of 8.95 km. Shallower depth usually correlates with higher geothermal gradients. For this reason, block 14 recorded the highest Geothermal Gradient of 61.77 °C/km and a heat flow value of 154.42 mW/m<sup>2</sup>, indicating areas where subsurface heat is closer to the surface. This is significant for geothermal exploration, as it suggests that this zone could be suitable for potential geothermal reservoirs. Conversely, the deeper Curie depths of 24.63km observed around Kwoi in Kaduna state (block 12) correlate with the lowest geothermal gradients, 22.42°C/km, and heat flow value of 56.04mW/m<sup>2</sup> observed for the study area. Furthermore, areas stretching from block 2 through block 12 to block 28, where water bodies form part of the surface geology, recorded the lowest heat flows for the study area. This could be attributed to the fact that water bodies, such as rivers, lakes, and wetlands, can act as thermal insulators, reducing heat flow from the Earth's interior to the surface (Jandaghian and Colombo, 2024). This phenomenon is due to the low thermal conductivity of water compared to the surrounding rocks. It could further be due to the fact that Central Nigeria is characterized by sedimentary basins, such as the Niger Delta and the Benue Trough. These basins are filled with low-thermal-conductivity sediments, which can reduce heat flow (Vosteen & Schellschmidt, 2003; Theissen and Rüpke, 2010). These findings are consistent with existing studies on central Nigeria, such as those by Yakubu *et al.* (2023) and Dimgba *et al.* (2020), which reported similar patterns in areas with varying geothermal potentials depending on the depth of the Curie isotherm.

Although the highest and lowest heat flow and geothermal gradient values were recorded at a distance not too far apart (blocks 12 and 14), the geothermal gradient and heat flow can vary significantly

over distances of only tens of kilometres due to local geologic settings (N'aslund *et al.*, 2005). The analysis of the geothermal gradient and heat flow from this study indicates a direct relationship between the Curie point depth and thermal properties. Areas around Anta, and areas stretching from Bwari, through Kagarko to parts of Kachia and Kafanchan (blocks 14,9,23,26 and 15) are associated with high geothermal gradients (typically above 40 °C/km) and elevated heat flow values (above 100 mW/m<sup>2</sup>). These values are comparable to regions identified in the Chad Basin and Benue Trough, where similar geothermal anomalies were observed (Dimgba *et al.*, 2020). Furthermore, Sharma (2004) points out that the minimum heat flow consideration for the generation of geothermal energy is 60 mW/m<sup>2</sup>. The study further posits that heat flow values ranging from 80 to 100 mW/m<sup>2</sup> indicate anomalous geothermal conditions, which can be caused by geological structures, fluid circulation, or human activities, and can signify potential geothermal resources, hydrothermal mineralizations, or geological hazards. Examples include Hot springs, geysers, and volcanic regions. Therefore, the high values recorded in these blocks suggest the presence of significant geothermal anomalies, making these blocks prime targets for further exploration and potential drilling activities. These findings are also consistent with studies by Aljubran and Horne (2024), which suggest geothermal gradient values above 40 °C/km to be significant even for enhanced geothermal systems (EGS).

## Conclusion

Aeromagnetic surveys have proven effective in geophysical explorations due to their ability to detect variations in the Earth's magnetic field caused by different rock types and thermal structures. The centroid method utilized in this study proved efficient for calculating the depth to the top ( $Z_t$ ), and centroid ( $Z_0$ ) of magnetic sources. Using these values, the heat flow and geothermal gradient were successfully calculated for the study area. The findings from this study indicate that parts of central Nigeria, as analyzed in this study, possess significant geothermal potential. Shallow Curie depths, high geothermal gradients, and elevated heat flow values identified in this study for areas such as Anta and Kaura position the area as promising for geothermal exploration. This highlights the importance of further geophysical surveys and exploratory drilling (ground-truthing) in the areas with prospects of high geothermal potential to assess their suitability for geothermal energy generation.

## REFERENCES

- Bernadette, C. D., Obiora, D. N., Abangwu, J. U., & Ugbor, D. O. (2020). Study of Curie point depth and heat flow from spectral analysis of aeromagnetic data for geothermal potential of Gubio, Chad Basin, Nigeria. *SN Applied Sciences*, 2, 1351. <https://doi.org/10.1007/s42452-020-03063-7>
- Bhattacharyya, B. K., & Leu, L. K. (1975). Spectral analysis of gravity and magnetic anomalies due to two-dimensional structures. *Geophysics*, 40(6), 993–1013. <https://doi.org/10.1190/1.1440593>
- Byerly, P. E., & Stolt, R. H. (1977). An attempt to define the Curie point isotherm in Northern and Central Arizona. *Geophysics*, 42(7), 1394–1400. <https://doi.org/10.1190/1.1440797>
- Dippio, R., & Renner, J. L. (2014). *Geothermal energy*. In T. M. Letcher (Ed.), *Future energy* (pp. 471–492). Elsevier. <https://doi.org/10.1016/B978-0-08-099424-6.00024-4>
- Dimgba, B. C., Obiora, D. N., Abangwu, J. U., & Ugbor, D. O. (2020). Study of Curie point depth and heat flow from spectral analysis of aeromagnetic data for geothermal potential of Gubio, Chad Basin, Nigeria. *SN Applied Sciences*, 2, 1–9. <https://doi.org/10.1007/s42452-020-03063-7>
- Geothermal Energy Association. (2012). *Geothermal basic questions and answers*. Geothermal Energy Association. [http://geo-energy.org/reports/Geothermal\\_Basics.pdf](http://geo-energy.org/reports/Geothermal_Basics.pdf)
- Glassley, W. E. (2010). *Geothermal energy: Renewable energy and the environment*. CRC Press.
- Jandaghian, Z., & Colombo, A. (2024). The role of water bodies in climate regulation: Insights from recent studies on urban heat island mitigation. *Buildings*, 14(9), 2945. <https://doi.org/10.3390/buildings14092945>
- Jimah, K. Q., Isah, A. W., & Okundamiya, M. S. (2019). Erratic and epileptic power supply in Nigeria: Causes and solutions. *Advances in Electrical and Telecommunication Engineering*, 2(1), 47–53.
- Kasidi, S., & Nur, A. (2012). Curie depth isotherm deduced from spectral analysis of magnetic data over Sarti and environs of North-Eastern Nigeria. *Scholars Journal of Biotechnology*, 1, 49–56.
- Langel, R. A., & Hinze, W. J. (1998). *The magnetic field of the lithosphere: The satellite perspective* (Vol. 429, pp. 157–158). Cambridge University Press.
- Nemzer, M. L., Carter, A. K., & Nemzer, K. P. (2009). Geothermal energy. In *Microsoft Encarta 2009* [DVD]. Microsoft Corporation.
- Odidi, G. I., Mallam, A., & Nasir, N. (2020). Determination of the Curie point depth, thermal gradient, and heat flow of parts of Central and North-Eastern Nigeria using spectral analysis technique. *Unpublished manuscript*.
- Odidi, I., Mallam, A., & Nasir, N. (2020). Investigation of geothermal energy potential of parts of Central and North-Eastern Nigeria using spectral analysis technique. *FUDMA Journal of Sciences*, 4(2), 627–638.
- Okubo, Y., Graf, R. J., Hansen, R. O., Ogawa, K., & Tsu, H. (1985). Curie point depths of the island of Kyushu and surrounding areas, Japan. *Geophysics*, 50(3), 481–494. <https://doi.org/10.1190/1.1441923>
- Onwuemesi, A. G. (1997). One-dimensional spectral analysis of aeromagnetic anomalies and Curie depth isotherm in the Anambra Basin of Nigeria. *Journal of Geodynamics*, 23(2), 95–107. [https://doi.org/10.1016/S0264-3707\(96\)00024-6](https://doi.org/10.1016/S0264-3707(96)00024-6)
- Sharma, P. V. (2004). *Environmental and engineering geophysics* (2nd ed., pp. 357–359). Cambridge University Press.
- Spector, A., & Grant, F. S. (1970). Statistical models for interpreting aeromagnetic data. *Geophysics*, 35(2), 293–302. <https://doi.org/10.1190/1.1440092>
- Stacey, F. D. (1977). *Physics of the Earth* (2nd ed.). Wiley.
- Stampolidis, A., Kane, I., Tsokas, G. N., & Tsourlos, P. (2005). Curie point depths of Albania inferred from ground total field magnetic data. *Surveys in Geophysics*, 26, 461–480. <https://doi.org/10.1007/s10712-005-3856-2>
- Theissen, S., & Rüpke, L. H. (2010). Feedbacks of sedimentation on crustal heat flow: New insights from the Vøring Basin, Norwegian Sea. *Basin Research*, 22(6), 976–

990. <https://doi.org/10.1111/j.1365-2117.2009.00450.x>
- Vosteen, H. D., & Schellschmidt, R. (2003). Influence of water content on thermal conductivity of sedimentary rocks. *Journal of Geophysics and Engineering*, 1(1), 44–52. <https://doi.org/10.1088/1742-2132/1/1/004>
- Yakubu, J. A., Amuche, I. D., Igwe, A. E., Shuaibu, A., & Okwesili, A. N. (2023). Investigation of Curie point depth using high-resolution aeromagnetic data of Igumale and Ejekwe Area, Lower Benue Trough, Nigeria. *Indian Journal of Science and Technology*, 16(8), 540–546. <https://doi.org/10.17485/IJST/v16i8.300>